Mem. S.A.It. Vol. 77, 834

Memorie della

The evolution of primordial Super–AGB stars

Enrique García–Berro[1,2], Pilar Gil–Pons[1] and Jordi Gutiérrez[1]

[1] Departament de Física Aplicada, Universitat Politècnica de Catalunya, Escola Politécnica Superior de Castelldefels, Av. del Canal Olímpic, s/n, 08860, Castelldefels, Spain
[2] Institut d'Estudis Espacials de Catalunya (IEEC), Ed. Nexus-201, c/ Gran Capità 2-4, 08034, Barcelona, Spain

Abstract. We compute and analyze the evolution of primordial stars of ZAMS masses between $6\,M_{\odot}$ and $10\,M_{\odot}$, with and without overshooting. Our calculations cover from the main sequence until the formation of the degenerate cores and the thermally pulsing phase. Our main goals are to determine the nature of the remnants of heavy–weight intermediate–mass primordial stars and to check the influence of overshooting in their evolution. In doing so, we have obtained the values for the limiting masses of Pop III progenitor stars leading to carbon–oxygen and oxygen–neon compact cores. Moreover, we have also obtained the limiting mass for which isolated primordial stars would lead to core–collapse supernovae after the end of the main central burning phases. Considering a moderate amount of overshooting shifts to lower values the mass thresholds at the ZAMS for the formation of carbon–oxygen and oxygen–neon degenerate cores by about $\sim 2\,M_{\odot}$. As a by–product of our calculations, we have obtained the structure and composition profiles of the resulting compact remnants and the properties of the thermal pulses.

Key words. stars: evolution — stars: AGB — stars: supernovae — stars: Pop III

1. Introduction

Primordial stars, that is, stars formed in the early Universe, are direct inheritors of the matter synhesized during the Big Bang. The initial composition of these stars, characterized by the absence of metals, determines their evolution and, ultimately, the fundamental properties of the resulting remnants, as well as the amount and composition of the matter returned to the interstellar medium after the main evolutionary phases. Therefore, the evolution of these stars is important for a correct modelling of the primordial population of degenerate remnants and, hence, for a deeper understanding of the distribution of baryonic dark matter, whereas the significance of the ejected material rests on its influence on galactic chemical evolution.

Even though the detection of primordial composition objects — stars with [Fe/H] ≈ -8.3 — has not been possible up to now, during the last few years several encouraging observations in this direction have been done. For instance Christlieb et al. (2002) measured the metallicity of HE 0107–5240, a low mass star with [Fe/H] ≈ -5.3. Even more recently, Frebel et al. (2005) have observed HE 1327–2326, with [Fe/H] ≈ -5.4. Consequently, both the intrinsic theoretical interest and the growing observational evidence for the existence of very metal poor stars make the study of these

Send offprint requests to: garcia@fa.upc.edu

objects one of the hottest topics in stellar astrophysics nowadays.

The evolution of $Z = 0$ stars has been analyzed in several recent publications. Just to mention some of them, and without trying to be complete, Heger et al. (2000) Heger & Woosley (2002) and Chieffi & Limongi (2002) focused on massive stars, whereas Marigo et al. (2001), Chieffi et al. (2001) and Siess et al. (2002) studied the evolution of low– and intermediate–mass stars. However, the evolution of heavy–weight intermediate–mass primordial stars has been largely ignored, except for the case of the evolutionary sequence of a 9 $M_{\odot}$ star presented in Gil–Pons et al. (2005). Probably, one of the reasons for this is the heavy computational load involved in computing the evolution during the carbon burning phase in this mass range (Ritossa et al. 1995; García–Berro et al. 1997; Iben et al. 1997; Ritossa et al. 1999). The situation is, however, quite different for Pop I and II stars. For instance, the mass thresholds for stars leading to different types of remnants have been determined by Heger et al. (2003), and by Eldridge & Tout (2004).

Here we describe the final stages of the evolution of heavy–weight intermediate–mass primordial stars. Reliable results on this topic are essential inputs for Galactic chemical evolution models, as well as for the supernova theory. Particularly, thermonuclear supernovae (SNeIa), in which a carbon–oxygen white dwarf overcomes the Chandrasekhar limit, must rely on accurate initial–to–final mass relations to reproduce the observed supernova rates. Moreover, a dependence of their properties on metallicity could represent a source of diversity at different look–back times. Specifically, we determine the mass thresholds to obtain carbon–oxygen (CO), oxygen–neon (ONe) degenerate cores and core collapse SNe at the end of the main central burning stages. The stars hosting CO degenerate cores could produce either CO novae or SNeIa if belonging to a close binary system; those stars hosting an ONe degenerate core could form ONe novae or SNe by the accretion–induced collapse mechanism (Canal & Schatzman 1976; Gutiérrez et al. 1996; Gutiérrez et al., 2005) and core–collapse SNe would directly form from isolated stars when nuclear burning proceeds all the way to the formation of an iron dominated core.

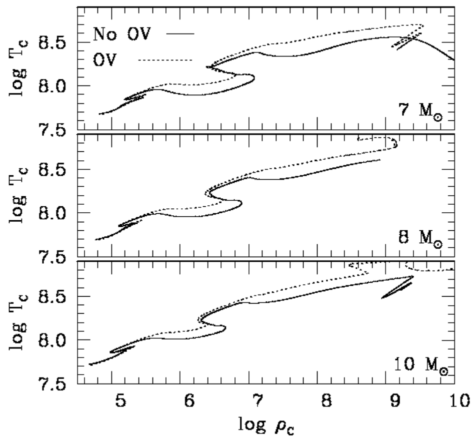

Fig. 1. Evolution in the $\log \rho_c - \log T_c$ plane of our model stars up to the point where carbon is ignited. The solid lines correspond to the cases without overshooting and the dotted lines correspond to the cases computed with overshooting.

The paper is organized as follows: in §2 we describe the overall evolution prior to carbon burning. The carbon burning phase is described in §3, wheras in §4 we present the thermally pulsing phase. Finally in §5 we summarize our conclusions.

2. Overall evolution prior to carbon burning

We have used the evolutionary code previously described in Gil–Pons et al. (2005). The only novelty is the incorporation of overshooting, that allows us to isolate the differences introduced by the treatment of the convective boundaries in our calculations. The prescription we have used for determining the convective edges is the one described in Eldridge & Tout (2004). The evolution prior to carbon burning follows the main trends previously described in Gil–Pons et al. (2005). That is, core hydrogen burning (CHB) begins through the pp–chains until small amounts of carbon

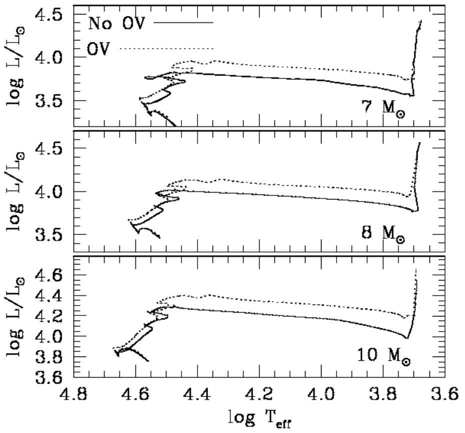

Fig. 2. Evolutionary track in the Hertzsprung–Russell diagram of our model stars. Again, solid lines correspond to the cases without overshooting and the dotted lines correspond to the cases computed with overshooting.

(X(C) = 10^{-10}) form and allow the onset of the CNO cycle. The rest of the CHB phase proceeds therefore at the higher central temperatures that characterize this cycle. Once CHB has ended, core contraction proceeds and the conditions for core helium burning (CHeB) are reached in the central regions of the star. Those for hydrogen burning are attained at the layers just above the H–exhausted core. However, hydrogen shell burning in a metal–free environment is not able to produce the overall expansion of the stellar envelope that characterizes the red giant branch.

The calculations with overshooting yield time scales for the CHB phase that are about ~12% longer when compared to the cases computed without taking overshooting into account. The helium cores after the CHB phase has been completed are also about ~50% larger, and this is the reason why CHeB lasts about ~6% longer in the cases in which overshooting was incorporated. Finally, the sizes of the CO cores prior to carbon burning are considerably larger as well, about ~25% more massive for the cases computed with overshooting.

Figure 1 shows the evolution of the central temperature versus the central density for the 7, 8 and 10 $M_\odot$ models with overshooting (solid lines) and with overshooting (dotted lines). As can be seen, only small differences appear between both sets of models during the CHB phase. However, the core contraction phase that follows the CHB and the CHeB phases take place at higher temperatures and reach lower values for the maximum central density in the cases computed with overshooting. The evolution in the Hertzsprung–Russell diagram of the same model stars is shown in figure 2. In the upper panel the track of the 7 $M_\odot$ star is shown, and in the middle and lower panel we represent the evolution of the 8 $M_\odot$ and 10 $M_\odot$ models, respectively. CHB takes place at higher effective temperatures for the models computed with overshooting, and the Hertzsprung gap occurs at larger luminosities. In summary, the models computed with overshooting behave as if they were more massive than their counterparts computed without overshooting.

3. The carbon burning phase

Figure 3 represents the time evolution of the base of the convective envelope (BCE) and the luminosities associated to carbon burning (thick line) and helium burning (thin line) for the 8 $M_\odot$ model stars, which are representative cases, computed without overshooting (top panel) and with overshooting (bottom panel). The convective regions associated to carbon burning are also shown for both models. We remark at this point that neither the 6 $M_\odot$ nor the 7 $M_\odot$ model stars computed without overshooting develop carbon burning extensively and, therefore, their cores are composed mainly of carbon and oxygen. In fact, our calculations show that the mass threshold at the ZAMS for effective carbon burning in the partially degenerate core to obtain an ONe core is $\approx$ 7.8 $M_\odot$, when no overshooting is considered. This mass threshold is $\approx$ 6.0 $M_\odot$ when overshooting is taken into account.

The first important feature to be noticed in Fig. 3 is the fast advance of the base of the convective envelope (BCE) that, for both mod-

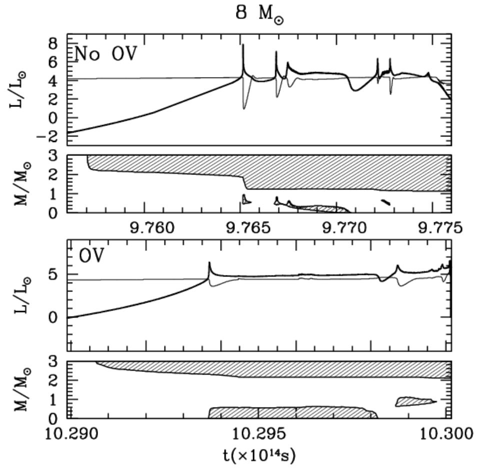

Fig. 3. Temporal evolution of the main structural parameters during the carbon burning phase for the 8 $M_\odot$ model computed with and without overshooting (upper an bottom panel, respectively). The shaded areas represent the convective regions, the thick line depicts the carbon luminosity, L_C, and the thin line corresponds to the helium luminosity, L_{He}.

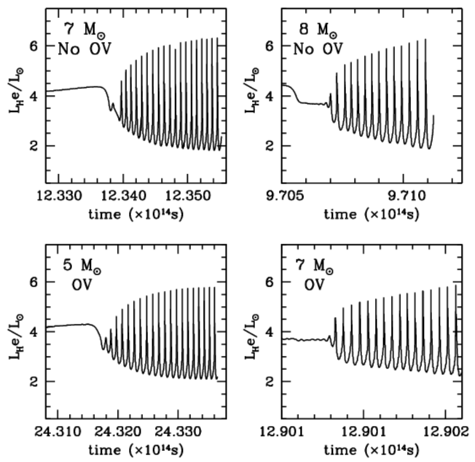

Fig. 4. Evolution of L_{He} during the early TP–AGB phase of the 7 $M_\odot$ model computed without overshooting, upper left panel, the 8 $M_\odot$ without overshooting, upper right panel, the 5 $M_\odot$ model computed with overshooting (lower left panel), and the 7 $M_\odot$ with overshooting (lower right panel).

els, occurs shortly after the end of the CHeB phase and the onset of helium burning in a shell This first advance inwards, the so–called "second" dredge–up episode — although, in fact, this is the first dredge–up episode — is followed by a very slow penetration of the BCE that finally allows for a moderate enrichment in metals of the hydrogen–rich envelope. This enrichment could have a key role in the final fate of heavy–weight intermediate–mass primordial stars. The 8 $M_\odot$ model star computed without overshooting shows a particular feature associated with the inner advance of the convective envelope. For this model the onset of the first carbon flash at $t \sim 9.766 \times 10^{14}$ s occurs relatively close to the BCE and, thus, allows for a decrease of the degeneracy parameter of the outermost layers of the core. Consequently, the density and temperature barriers decrease and this results in an additional advance of the BCE. This, in turn, produces a significant enrichment in metals of the convective envelope. For the model computed with overshooting this feature is absent, since carbon ignition occurs at the center, too far from the edge of the carbon–oxygen partially degenerate core to have appreciable consequences in the behavior of the convective envelope.

4. The thermally pulsing phase

In figure 4 we present the behavior of the helium luminosity for the first few thermal pulses for some selected models. The fact that these stars develop the TP–(S)AGB phase in a way similar to that of their solar metallicity counterparts of analogous masses is a consequence of the previous dredge–up processes that occur during the activation of the helium burning shell. The associated metal enrichment of the hydrogen–rich convective envelope, as well as the heating of its base due to the proximity of the helium burning shell (HeBS), allow for the reignition of hydrogen through the CNO–cycle. This occurs when the distance between the HeBS and the BCE is of about 10^{-4} $M_\odot$.

Figure 5 shows the sizes and compositions of the remnant cores at the end of our calculations. Those cores with masses larger than the Chandrasekhar mass at the beginning of

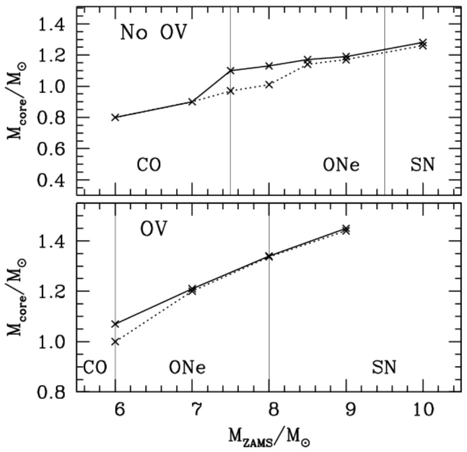

Fig. 5. Size of the final compact remnant core without overshooting (upper panel) and without it (lower panel).

the carbon burning phase have been assumed to undergo a direct SN explosion. It is important to realize that although we have followed a significant number of thermal pulses we have not found any dredge–up during the TP–(S)AGB phase. This fact would have important consequences regarding the time scales for the ejection of the hydrogen–rich envelope, as stellar winds are expected to depend on metallicity according to the relation:

$$\dot{M}(Z) = \dot{M}(Z_\odot)\left(\frac{Z}{Z_\odot}\right)^{0.5} \tag{1}$$

where $\dot{M}(Z_\odot)$ is the mass–loss rate for solar metallicity, for which we have adopted the prescription of Reimers (1975).

In figure 6 we have represented the metallicity of the envelope, Z_{env} for some of our models at the end of our calculations (lower panel), and the expected mass–loss rates according to Eq. (1). If we use these metallicities to compute the time required for the star to get deprived of the envelope we get the values shown in columns 3 — without the effect of Z_{env} — and 4 — computed scaling the mass–loss rate as the square root of the metallicity — of table 1. For the sake of comparison, we also show in column 2 the time required for the core

Table 1. Time scales (in Myr) associated to core growth and loss of the envelope without overshooting (top section) and with overshooting (bottom section).

$M_{ZAMS}/M_\odot$	t_{core}	t_{env}	$t_{env}(Z)$
6	2.0	50	2.0×10^4
7	1.0	60	6.0×10^3
8	0.8	70	0.8×10^3
6	0.9	80	2.0×10^5
7	1.2	90	7.0×10^4
8	1.2	120	3.6×10^3

to grow up to the Chandrasekhar mass (M_{Ch}). The fact that the latter values are considerably lower than the expected time scales required to lose the stellar envelope casts serious doubts on the final fate of intermediate–mass primordial stars and leaves the possibility open for the formation of SNIe1/2 (Zijlstra 2004).

5. Conclusions

The evolution of heavy–weight intermediate–mass primordial stars has been followed from the main sequence until the early stages of the TP–(S)AGB phase. We have performed our calculations both without and with a moder-

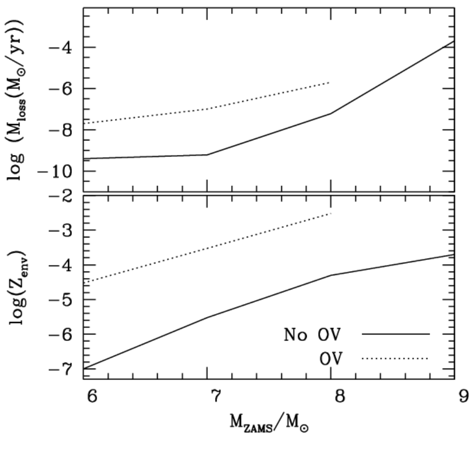

Fig. 6. Lower panel: metallicity of the envelope for some of our models at the end of our calculations. Upper panel: expected mass losses given the former metallicities.

ate amount of overshooting and, therefore, we have been able to determine its main effects on the overall evolution. As a summary, taking overshooting into account causes longer CHB and CHeB phases and the developement of cores whose mass, structure and composition are similar to those of stars of ZAMS mass $2\,M_{\odot}$ higher than those computed without overshooting. In particular, the minimum mass required to develop extensive carbon burning is lowered from $7.8\,M_{\odot}$ to $6\,M_{\odot}$ but, on the other hand, the standard pattern of strong carbon flashes and associated convective shells is followed in all cases, as it occurs for heavy–weight intermediate–mass stars of solar metallicity. As to the dredge–up processes, we have found that they occur as a consequence of the onset of the HeBS, and checked that the pollution of the outer envelope is higher for the more massive models. This dredge–up allows enough enrichment in carbon of the base of the envelope for a new onset of the HBS that, in this case, develops through the CNO cycle and, therefore, the subsequent TP–(S)AGB phases take place in a way similar to that of solar metallicity stars. On the other hand, during the TP–(S)AGB phase we have found that the dredge–up is not enough to increase significantly the metallicity of the envelope. Using the data from our models and the parametrization of Reimers (1975) for the mass losses we have found that the time expected for the cores of our models to reach M_{Ch} is much smaller than the time expected for the removal of the envelopes and, therefore, our model stars might end their lives as SNIe1/2.

Acknowledgements. This work has been partially supported by the MCYT grant AYA2005–08013–C03–01, by the AGAUR and by the European Union FEDER funds.

References

Abia, C., Domínguez, I., Straniero, O., Limongi, M., Chieffi, A., & Isern, J., 2001, ApJ, **557**, 126

Canal, R., Schatzman, E., 1976, A&A, **46**, 229

Chieffi, A., Domínguez, I., Limongi, M., & Straniero, O., 2001, ApJ, **554**, 1159

Chieffi, A., & Limongi, M., 2002, ApJ, 577, 281

Christlieb, N., Bessell, M.S., Beers, T.C., Gustafsson, B., Korn, A., Barklem, P.S., Karlsson, T., Mizuno–Wiedner, M., & Rossi, S., 2002, Nature, **419**, 904

Eldridge, J.J., & Tout, C.A., 2004, MNRAS, **353**, 87

Frebel, A., Aoki, W., Christlieb, N., Ando, H., Asplund, M., Barklem, P.S., Beers, T.C., Eriksson, K., Fechner, C., Fujimoto, M.Y., Honda, S., Kajino, T., Minezaki, T., Nomoto, K., Norris, J.E., Ryan, S.G., Takada-Hidai, M., Tsangarides, M., Yoshii, Y., 2005, Nature, **434**, 871

García–Berro, E., Ritossa, C., & Iben, I., 1997, ApJ, **485**, 765

Gil–Pons, P., Suda, T., Fujimoto, M.Y., & García-Berro, E., A&A, **433**, 1037

Gorieli, S., & Siess, L., 2001, A&A, **378**, 25

Gutiérrez, J., García-Berro, E., Iben, I., Isern, J., Labay, J., Canal, R., 1996, ApJ, **459**, 701

Gutiérrez, J., Canal, R., García-Berro, E., 2005, A&A, **435**, 231

Heger, A., & Woosley, S.E., 2002, ApJ, **567**, 532

Heger, A., Woosley, S.E., & Waters, R., 2000, in *"The First Stars"*, Eds.: A. Weiss, T.G. Abel, & V. Hill, (Springer: Berlin), 121

Heger, A., Fryer, C.L., Woosley, S.E., Langer, N., Hartmann, D.H., 2003, ApJ, **591**, 288

Iben, I., Ritossa, C., & García–Berro, E., 1997, ApJ, **489**, 772

Iglesias, C.A., & Rogers, F.J., 1993, ApJ, **412**, 752

Marigo, P., Girardi, C., Chiosi, C., & Wood, R., 2001, A&A, **371**, 152

Reimers, D., 1975, Mem. Soc. R. Sci. Liège, ser. 6, **8**, 369

Ritossa, C., García–Berro, E., & Iben, I., 1995, ApJ, **460**, 489

Ritossa, C., García–Berro, E., & Iben, I., 1999, ApJ, **515**, 381

Siess, L., Livio, M., Lattanzio, J., 2002, ApJ, **570**, 329

Schroeder, K.P., Pols, O.R., & Eggleton, P.P., 1997, MNRAS, **285**, 696

Zijlstra, A.A., 2004, MNRAS, **348**, L23